Multistage Generation and Network Expansion Planning in Distribution Systems Considering Uncertainty and Reliability

Gregorio Muñoz-Delgado, *Student Member, IEEE*, Javier Contreras, *Fellow, IEEE*, and José M. Arroyo, *Senior Member, IEEE*

***Abstract*—This paper describes the incorporation of uncertainty and reliability in the dynamic expansion planning of distribution network assets and distributed generation. Several alternatives for the installation of feeders, transformers, and distributed generation are considered. Thus, the optimal expansion plan identifies the best alternative, location, and installation time for the candidate assets under the uncertainty related to demand and renewable energy sources. To that end, an iterative algorithm is devised to yield a pool of high-quality candidate solutions in terms of total investment and operational costs. Each candidate solution results from a stochastic-programming-based model driven by the minimization of the expected investment and operational costs. The associated scenario-based deterministic equivalent is formulated as a mixed-integer linear program for which finite convergence to optimality is guaranteed and efficient off-the-shelf software is available. Standard metrics are subsequently applied to each candidate solution to characterize its reliability so that valuable information is provided to the distribution system planner. Numerical results illustrate the effective performance of the proposed approach.**

***Index Terms*—Distributed generation, distribution system planning, multistage, network expansion, reliability, stochastic programming, uncertainty.**

NOMENCLATURE

A. Indices

b	Index for time blocks.
h	Index for the blocks used in the piecewise linearization of energy losses.
i, j, r	Indices for nodes.
k, κ	Indices for available investment alternatives.
l	Index for feeder types.
m, ϱ	Indices for iterations.
p	Index for generator types.
s	Index for segments dividing the cumulative distribution functions.
t, τ	Indices for time stages.
tr	Index for transformer types.
γ	Index for interruption types.
ω	Index for scenarios.

B. Sets

B	Index set of time blocks.
K^l, K^p, K^{tr}	Index sets of available alternatives for feeders, generators, and transformers.
L	Set of feeder types. $L = \{EFF, ERF, NRF, NAF\}$ where EFF, ERF, NRF, and NAF denote existing fixed feeder, existing replaceable feeder, new replacement feeder, and newly added feeder, respectively.
P	Set of generator types. $P = \{C, W, \Theta\}$ where C, W, and Θ stand for conventional, wind power, and photovoltaic generation, respectively.
T	Index set of time stages.
TR	Set of transformer types. $TR = \{ET, NT\}$ where ET and NT denote existing transformer and new transformer, respectively.
Γ	Set of interruption types. $\Gamma = \{RP, SW\}$ where RP and SW stand for repair and switching, respectively.
$\Lambda^{0(\varrho)}, \Lambda^{1(\varrho)}$	Sets of branches with candidate feeders for addition where no investments and investments have been respectively made at iteration ϱ.
$\Upsilon^l, \Upsilon^{SW,l}$	Set of branches with feeders of type l and subset of those branches with switchable feeders under normal operation.

Manuscript received March 20, 2015; revised July 16, 2015 and October 16, 2015; accepted November 21, 2015. Date of publication December 11, 2015; date of current version August 17, 2016. This work was supported in part by the European Union 7th Framework Programme FP7/2007–2013, under Grant 309048, Project SiNGULAR, the Ministry of Science of Spain, under CICYT Project ENE2012-30679, the Junta de Comunidades de Castilla-La Mancha, under Project POII-2014-012-P and Grant PRE2014/8064, and the Universidad de Castilla-La Mancha, under Grant GI20152945. Paper no. TPWRS-00387-2015.

The authors are with the Escuela Técnica Superior de Ingenieros Industriales, Universidad de Castilla-La Mancha, 13071 Ciudad Real, Spain (e-mail: gregorio.munoz.delgado@gmail.com; Javier.Contreras@uclm.es; JoseManuel.Arroyo@uclm.es).

Digital Object Identifier 10.1109/TPWRS.2015.2503604

Υ_t Set of branches with a feeder at stage t.

$\Psi_i^l, \Psi_t^{LN}, \Psi^N, \Psi^p, \Psi^{SS}$ Index sets of nodes connected to node i by a feeder of type l, load nodes, system nodes, candidate nodes for distributed generation, and substation nodes.

Ψ_{ijt}^{γ} Index set of nodes affected by an interruption of type γ due to a fault in the feeder connecting nodes i and j at stage t.

Ω_b Set of scenarios for time block b.

C. Parameters

A_{kh}^l, A_{kh}^{tr} Width of block h of the piecewise linear energy losses for feeders and transformers.

$ASAI_t$ Average system availability index for stage t.

$C_k^{E,p}, C_b^{SS}, C^U$ Cost coefficients of energy supplied by generators and substations, and unserved energy.

$C_k^{I,l}, C_k^{I,NT}, C_k^{I,p}, C_i^{I,SS}$ Investment cost coefficients of feeders, new transformers, generators, and substations.

$C_k^{M,l}, C_k^{M,p}, C_k^{M,tr}$ Maintenance cost coefficients of feeders, generators, and transformers.

CIC_t Cost of customer interruption at stage t.

CIC^{PV} Present value of the cost of customer interruption.

$\overline{CID}$ Target for the customer interruption duration.

CID_{it} Customer interruption duration at node i and stage t.

$CIDC_t$ Cost of customer interruption duration at stage t.

$\overline{CIF}$ Target for the customer interruption frequency.

CIF_{it} Customer interruption frequency at node i and stage t.

$CIFC_t$ Cost of customer interruption frequency at stage t.

$D_{it}, \tilde{D}_{it}$ Actual nodal peak demand and fictitious nodal demand.

$D_{itb}^{net}(\omega)$ Net demand at node i and stage t for time block b and scenario ω.

DI^{γ} Duration of interruption type γ.

$EENS_t$ Expected energy not supplied at stage t associated with feeder outages.

$EENSC_t$ Cost of the expected energy not supplied at stage t associated with feeder outages.

$EENSC^{PV}$ Present value of the cost of the expected energy not supplied associated with feeder outages.

$\bar{F}_k^l$ Upper limit for actual current flows through feeders.

$\bar{G}_k^p, \hat{G}_{ikb}^p(\omega)$ Rated capacities of generators and maximum power availability.

$\bar{G}_k^{tr}$ Upper limit for current injections of transformers.

I Annual interest rate.

IB_t Investment budget for stage t.

J Sufficiently large positive constant.

ℓ_{ij} Feeder length.

M_{kh}^l, M_{kh}^{tr} Slope of block h of the piecewise linear energy losses for feeders and transformers.

n_B, n_T, n_Ω Number of time blocks, number of time stages, and number of scenarios per time block.

n_d Minimum number of topology differences among expansion plans.

n_{DG}, n_H Number of candidate nodes for installation of distributed generation and number of blocks of the piecewise linear energy losses.

n_S^D, n_S^p Number of segments for demand factors and number of segments for factors for generation of type p at each time block.

NC_{it} Total number of customers at node i and stage t.

pf System power factor.

$RR^l, RR^{NT}, RR^p, RR^{SS}$ Capital recovery rates for investment in feeders, new transformers, generators, and substations.

$SAIC_t$ Cost of system average interruption at stage t.

$SAIC^{PV}$ Present value of the cost of system average interruption.

$\overline{SAIDI}$ Target for the system average interruption duration.

$SAIDI_t$ System average interruption duration at stage t.

$\overline{SAIFI}$ Target for the system average interruption frequency.

$SAIFI_t$ System average interruption frequency at stage t.

$\underline{V}, \overline{V}$ Lower and upper bounds for nodal voltages.

$x_{ijkt}^{NAF(\varrho)}$ Value of variable x_{ijkt}^{NAF} at iteration ϱ.

$\hat{x}_{ikt}^p$ Given value of variable x_{ikt}^p.

Z_k^l, Z_k^{tr} Unitary impedance magnitude of feeders and impedance magnitude of transformers.

Δ_b Duration of time block b.

λ_{ij}	Average failure rate of the feeder connecting nodes i and j.
$\eta^l, \eta^{NT}, \eta^p, \eta^{SS}$	Lifetimes of feeders, new transformers, generators, and substation assets other than transformers.
μ^D_{sb}, μ^p_{sb}	Average factors for demand and generation for segment s.
$\mu^D_b(\omega)$	Average demand factor of time block b and scenario ω.
ξ	Penetration limit for distributed generation.
π^D_{sb}, π^p_{sb}	Probabilities of the average factors for demand and generation in segment s.
$\pi_b(\omega)$	Probability of scenario ω of time block b.
ς, χ	Penalty factors.

D. Variables

$c^E_t, c^M_t, c^R_t, c^U_t$	Expected costs of production, maintenance, energy losses, and unserved energy.
c^I_t	Amortized investment cost.
c^{TPV}	Present value of the expected total cost.
$d^U_{itb}(\omega)$	Nodal unserved energy.
$f^l_{ijktb}(\omega), \tilde{f}^l_{ijkt}$	Actual and fictitious current flows through feeders.
$g^p_{iktb}(\omega), g^{tr}_{iktb}(\omega), \tilde{g}^{SS}_{it}$	Current injections corresponding to generators and transformers, and fictitious current injection at substation nodes.
$v_{itb}(\omega)$	Nodal voltage magnitude.
$x^l_{ijkt}, x^{NT}_{ikt}, x^p_{ikt}, x^{SS}_{it}$	Binary investment variables for feeders, new transformers, generators, and substations.
$y^l_{ijkt}, y^p_{ikt}, y^{tr}_{ikt}$	Binary utilization variables for feeders, generators, and transformers.
$\delta^l_{ijktbh}(\omega), \delta^{tr}_{iktbh}(\omega)$	Current in block h of the piecewise linear energy losses for feeders and transformers.

I. Introduction

MULTISTAGE distribution system planning has been traditionally implemented by distribution companies within a centralized framework with the ultimate goal of meeting the growing demand along the planning horizon within quality standards and in a secure fashion [1]. Therefore, planning models are devised to obtain an optimal investment plan at minimum cost while complying with the security and quality requirements. Conventional planning models have typically determined the optimal expansion of distribution network assets including the replacement and addition of feeders, the reinforcement of existing substations and construction of new substations, and the installation of new transformers [1]–[3]. However, practical experience reveals that most service interruptions take place at the distribution level [4]. Therefore, further emphasis should be placed on the relevance of reliability in distribution system planning. Furthermore, the widespread growth of distributed generation (DG), mainly due to its numerous operational and planning benefits [4] and to the impetus of renewable energy, inevitably requires the inclusion of this kind of generation in distribution planning models [3], [5].

In the new context of co-optimized distribution system planning, uncertainty and reliability play key roles, thereby requiring particular attention. The increasing penetration of non-dispatchable renewable-based technologies for DG, such as wind and photovoltaic (PV) energy, calls for the inclusion of the uncertainty associated with the high variability of these energy sources, which is strongly dependent on the meteorology. Furthermore, load demand is another source of uncertainty with large impact on generation. Moreover, given the potential advantages of DG in terms of distribution reliability improvement [4], which are dependent on the location and sizing of these assets [6], reliability aspects have become essential drivers of the co-optimized expansion planning problem. Notwithstanding, the reliability improvement associated with renewable-based DG may be compromised due to the intermittency of the energy sources. Thus, uncertainty and reliability should be jointly considered in the new distribution system planning framework.

To the best of our knowledge, little attention has been paid so far to such joint consideration in the extensive literature on multistage distribution system planning including DG [3], [5], being relevant exceptions [7]–[11].

In [7], a genetic algorithm based on a probabilistic load flow was applied. Uncertainty was modeled through different scenarios of load demand and wind power generation according to a probability density function. In addition, based on the expected cost of energy not supplied and several standard indices, reliability was assessed in two phases, namely fault location and fault repair.

In [8], uncertainties in demand and DG were also represented through multiple scenarios. However, rather than optimizing over a set of scenarios, the expansion planning was solved for each scenario on an individual basis through the application of a genetic-algorithm-based approach. Subsequently, a heuristic decision-making process was implemented to yield a single expansion plan taking into consideration the scenario-dependent plans and their probabilities of occurrence. Reliability indices and the expected cost of energy not supplied were calculated by an analytical method considering both DG units and all protection devices installed in the distribution network.

In [9], uncertain wind power generation was modeled as a multistate variable by a probability density function. The use of a genetic algorithm allowed assessing reliability by the calculation of nodal interruption costs based on Monte Carlo simulation.

Finally, in [10] and [11], another evolution-inspired heuristic, namely evolutionary particle swarm optimization, was applied. Uncertainty related to load and electricity price was modeled through Monte Carlo simulation, whereas the failure mode and effect analysis was employed to quantify the energy not supplied.

The difficulty of incorporating reliability into distribution expansion planning models stems from the need to know the network topology in order to calculate (i) the reliability indices that characterize the system, and (ii) the operation under contingency, which is also topology dependent. However, the optimal network topology is an outcome of the optimization process characterizing the expansion planning problem wherein reliability is part of the model. As a consequence of this catch-22 conundrum, researchers have resorted to using metaheuristics [7]–[11] where a population of candidate plans is iteratively handled without being able to acknowledge optimality. In contrast, methods based on standard mathematical programming are currently unavailable in the technical literature and, hence, new approaches are yet to be explored.

In this paper, we propose a novel two-step algorithm to incorporate uncertainty and reliability in the multistage joint expansion planning model. First, a cost minimization model explicitly characterizing uncertainty is iteratively used to obtain a pool of low-cost expansion plans with different topologies. In this model, a scenario-based stochastic programming framework [12] is used to minimize the present value of the expected investment and operational costs under the correlated uncertainty of renewable-based generation and demand.

Subsequently, standard reliability indices [2], [13]–[16] and their associated reliability costs [16] are calculated for each solution of the pool. This information allows the decision maker to analyze the impact of reliability on the distribution expansion planning problem so that the most convenient investment is selected.

The proposed approach relies on the application of (i) a scenario-based stochastic programming framework [12], which is suitable to properly incorporate uncertainty in distribution system planning through the minimization of the present value of the expected total cost over a set of scenarios, as done in [7], [9]–[11]; (ii) a scenario-generation procedure relying on that successfully applied in [17] for demand and wind uncertainties, which has been extended to incorporate the uncertainty of solar irradiation, and which is suitable to properly characterize the correlated uncertainty associated with demand, wind power generation, and PV generation; (iii) a mixed-integer linear formulation for the expansion planning of both DG and distribution assets [18], which guarantees finite convergence to optimality while providing a measure of the distance to the optimum along the solution process [19], and for which efficient off-the-shelf software is readily available [20]; (iv) the contingency-enumeration-based reliability assessment described in [21], which has been adapted to incorporate the effect of both conventional and intermittent renewable-based DG; and (v) an iterative algorithm [16] that allows considering the effect of reliability on a pool of candidate cost-driven expansion plans.

Thus, the novelty of the proposed approach stems from collecting, extending, and integrating the valuable features of [12], [16]–[18], [21], which gives rise to an original, systematic, and effective solution approach that significantly differs from the state of the art [7]–[11] both from the modeling and methodological perspectives.

TABLE I
COMPARISON OF MULTISTAGE CO-OPTIMIZED EXPANSION PLANNING MODELS CONSIDERING UNCERTAINTY AND RELIABILITY

Approach	Topological changes	Photovoltaic generation	Correlation	Mathematical-programming-based
[7]	×	×	✓	×
[8]	✓	×	×	×
[9]	×	×	×	×
[10], [11]	×	×	×	×
Proposed approach	✓	✓	✓	✓

Unlike [7]–[11], where the topology of the network was either unchanged or slightly modified, substantial topological changes are allowed by modeling the installation of feeders in new branches and by modeling network reconfiguration under normal operation through feeder switching. It is worth mentioning that network reconfiguration plays a crucial role in the new context of smart distribution grids. Moreover, it should be emphasized that the consideration of topological changes complicates the optimization because specific constraints are required to impose radial operation and avoid the issues associated with islanded DG and transfer nodes. Another salient feature of the proposed approach is the consideration of both wind power generation and PV generation. Note that wind power generation was neglected in [10], [11], whereas PV generation was disregarded in [7]–[11].

Major distinctive aspects are also related to uncertainty modeling. In contrast to [8], where uncertainty was characterized by a rather low number of scenarios without prescribing the scenario-generation procedure, a systematic and effective methodology is proposed here to generate a sufficiently large number of scenarios so that a tradeoff between accuracy and computational tractability is materialized. Moreover, the proposed scenario-generation procedure is particularly tailored to account for the correlation among uncertainty sources, that was neglected in [8]–[11]. To that end, the method successfully applied in [17] to model the correlated uncertainty between demand and wind speed is here extended in an original fashion to also incorporate solar irradiation.

From a methodological viewpoint, rather than the heuristic scenario-based technique implemented in [8], a sound stochastic programming framework driven by expected cost minimization [12] is applied. Moreover, instead of the metaheuristics used in [7]–[11], that neither acknowledge global optimality nor provide a measure of the distance to the optimum, mixed-integer linear programming [19] is applied within an iterative framework [16] to yield a pool of candidate solutions for which reliability is straightforwardly assessed.

Table I summarizes the main differences between this paper and the state of the art [7]–[11]. In this table, symbols "✓" and "***X***" respectively indicate whether a particular aspect is considered or not.

The main contributions of this paper are as follows:

1) The distribution system planner is provided with a novel approach to make informed decisions on multistage co-op-

timized distribution system expansion planning based on both costs and reliability.

2) A scenario-based stochastic programming framework is proposed to model the correlated uncertainty characterizing demand and renewable-based power generation. The associated deterministic equivalent is formulated as a mixed-integer linear program suitable for commercially available software.
3) Rather than providing a single candidate plan, a pool of cost-effective solutions is given for which reliability is assessed by explicitly considering uncertainty in demand and renewable-based DG.

Regardless of the ownership of DG assets, the proposed approach provides valuable information about the best investment plan in terms of both economic and reliability factors. In the case of DG owned by independent producers, such information may be used to devise appropriate incentive strategies, which are beyond the scope of this paper.

The rest of this paper is organized as follows. In Section II, uncertainty modeling is characterized. In Section III, the stochastic programming model for cost minimization is formulated. Reliability indices and the associated costs are described in Section IV. Section V outlines the proposed two-step algorithm for co-optimized distribution system planning considering uncertainty and reliability. In Section VI, numerical experience is reported. Finally, some relevant conclusions are drawn in Section VII.

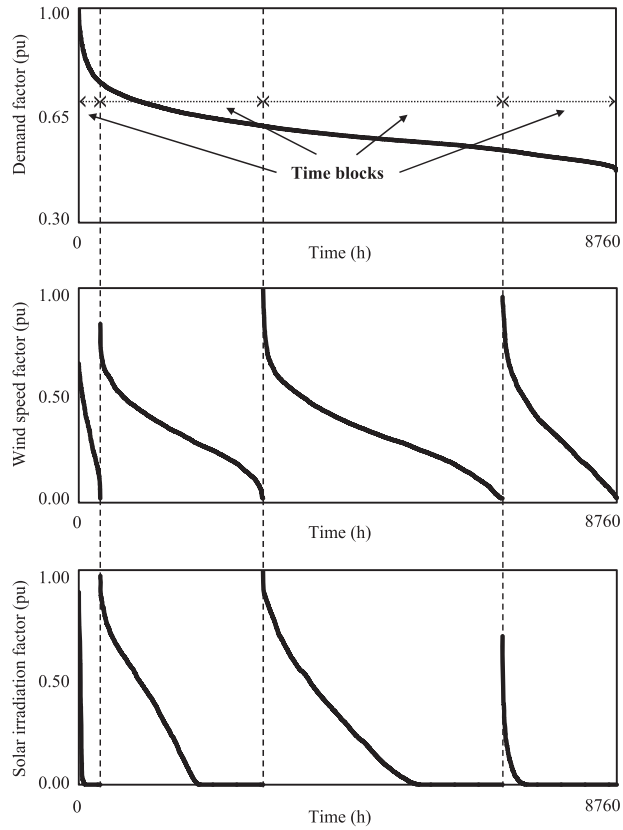

Fig. 1. Time block discretization of demand, wind speed, and solar irradiation factors.

II. Uncertainty Modeling

In the presence of renewable-based DG, multistage investment planning faces two major sources of uncertainty, namely demand and intermittent energy sources. Here, we propose characterizing the variability of demand, wind speed, and solar irradiation through a scenario-based stochastic programming framework [12]. The set of scenarios is built on historical data through the methodology described in [17]. Demand, wind speed, and solar irradiation are not statistically independent magnitudes. Thus, their statistical interrelations are specifically accounted for while maintaining the correlation among them. The proposed methodology comprises six steps that are described as follows.

Step 1) Historical hourly data of system demand, wind speed, and solar irradiation throughout a year are expressed as per-unit factors by dividing each of them by their corresponding maximum level (peak demand, maximum value of wind speed, and maximum value of solar irradiation).

Step 2) Triplets of hourly factors for demand, wind speed, and solar irradiation are sorted by demand factor in descending order.

Step 3) The factor curves resulting from step 2 are discretized into n_B time blocks. In order to accurately model the effect of the peak demand, which usually has a great influence on investment decisions, a relatively small time block is defined. For each time block, the corresponding wind speed and solar irradiation factors are sorted in descending order. An example with a 4-time-block discretization is depicted in Fig. 1.

Step 4) For each time block, the cumulative distribution functions (cdf) of the ordered demand, wind speed, and solar irradiation factors are built. Fig. 2 shows the cdfs corresponding to the curves depicted in Fig. 1.

Step 5) Each cdf is divided into a pre-specified number of segments with their corresponding probabilities, which are also user-defined parameters. The pre-specified numbers of segments for demand, wind speed, and solar irradiation factor curves are denoted by n_S^D, n_S^W, and n_S^Θ, respectively. For each cdf, in addition to its pre-specified probability π_{sb}^D, π_{sb}^W, or π_{sb}^Θ, each segment s is characterized by an average factor equal to the average value of the factors within this segment. As a consequence, probability-average factor pairs are generated for demand, namely $\pi_{sb}^D - \mu_{sb}^D$; for wind speed, namely $\pi_{sb}^W - \mu_{sb}^W$; and for solar irradiation, namely $\pi_{sb}^\Theta - \mu_{sb}^\Theta$. As an example, Fig. 3 shows the cdf of the first time block for the demand factor curve in Fig. 2, which is divided into three segments with probabilities, π_{11}^D, π_{21}^D, and π_{31}^D, equal to 0.4, 0.5, and 0.1, respectively. The demand factors associated with the segments respectively lie in the intervals [0.00, 0.70], (0.70, 0.86], and (0.86, 1.00]. For the cdf shown in Fig. 3, the corresponding average demand factors, μ_{11}^D, μ_{21}^D, and μ_{31}^D, are equal to 0.67, 0.76, and 0.90, respectively.

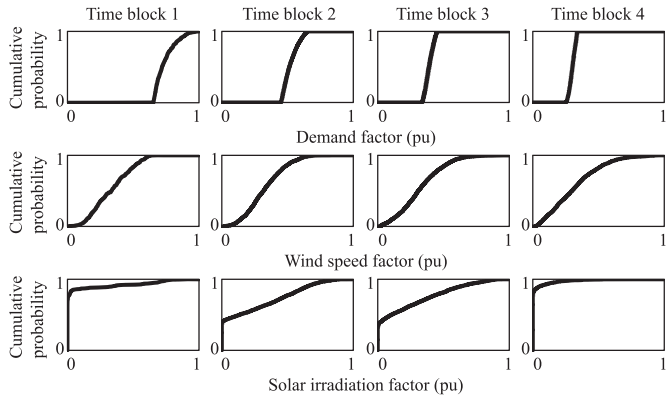

Fig. 2. Cumulative distribution functions of demand, wind speed, and solar irradiation factors.

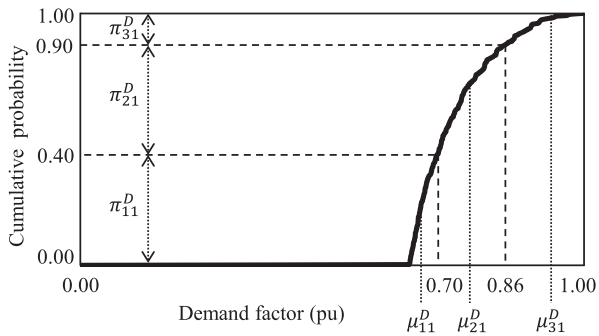

Fig. 3. Cumulative distribution function for the first block of the demand factor curve.

Step 6) Scenarios for each time block result from combining all pairs $\pi^D_{sb}-\mu^D_{sb}$, $\pi^W_{sb}-\mu^W_{sb}$, and $\pi^\Theta_{sb}-\mu^\Theta_{sb}$. Thus, for each scenario ω of time block b, the average demand factor $\mu^D_b(\omega)$ is equal to the value of μ^D_{sb} giving rise to such scenario. Nodal demands in each scenario are equal to the product of the forecasted values and the demand factor $\mu^D_b(\omega)$ throughout the planning horizon. Moreover, for each scenario ω, based on the information provided by the manufacturer, the corresponding average factors μ^W_{sb} and μ^Θ_{sb} are converted to maximum levels of wind and PV power generation, $\hat{G}^W_{ikb}(\omega)$ and $\hat{G}^\Theta_{ikb}(\omega)$, respectively. For the sake of simplicity, we consider that μ^W_{sb} and μ^Θ_{sb} are identical for all candidate nodes and that ambient temperature lies within a narrow range. Thus, for each time block b, scenario ω comprises an average demand factor, $\mu^D_b(\omega)$, a vector of maximum levels of wind power generation, $\hat{G}^W_{ikb}(\omega)$, and a vector of maximum levels of PV power generation, $\hat{G}^\Theta_{ikb}(\omega)$. Mathematically, the set of scenarios Ω_b is formulated as follows:

$$\Omega_b = \left\{ \mu^D_b(\omega), \left\{\hat{G}^W_{ikb}(\omega)\right\}_{\forall i\in\Psi^W,\ \forall k\in K^W}, \left\{\hat{G}^\Theta_{ikb}(\omega)\right\}_{\forall i\in\Psi^\Theta,\ \forall k\in K^\Theta} \right\}_{\forall\omega=1\ldots n_\Omega};\ \forall b\in B. \quad (1)$$

In addition, the probability of scenario ω of time block b, $\pi_b(\omega)$, is equal to the corresponding product $\pi^D_{sb}\pi^W_{sb}\pi^\Theta_{sb}$. The number of scenarios per time block, n_Ω, is equal to $n^D_S n^W_S n^\Theta_S$, whereas the number of scenarios or operating conditions per stage is equal to $n_B n_\Omega$.

III. Stochastic Programming Model

The proposed co-optimized expansion planning model is formulated as an instance of stochastic programming [12] where the correlated uncertainty of demand, wind power, and PV power is characterized by a set of scenarios. The proposed model is built on the deterministic formulation described in [18] wherein: (i) a multistage planning framework is adopted, (ii) the annual load curve is discretized into several time blocks, (iii) radial operation of the distribution network is explicitly imposed, (iv) an approximate network model is used, (v) the costs of losses are included in the objective function, and (vi) several investment alternatives exist for each asset. As done in previous works on multistage joint expansion planning considering both uncertainty and reliability [7]–[11], demand response is disregarded.

Based on [12], the stochastic programming model can be mathematically formulated as a scenario-based deterministic equivalent, as described next.

A. Objective Function and Cost-Related Terms

The goal of the proposed co-optimized model is the minimization of the present value of the expected total cost:

$$\begin{aligned} c^{TPV} = &\sum_{t\in T}\frac{(1+I)^{-t}}{I}c^I_t \\ &+\sum_{t\in T}\left[(1+I)^{-t}\left(c^M_t+c^E_t+c^R_t+c^U_t\right)\right] \\ &+\frac{(1+I)^{-n_T}}{I}\left(c^M_{n_T}+c^E_{n_T}+c^R_{n_T}+c^U_{n_T}\right). \end{aligned} \quad (2)$$

As done in [16], [18], the total cost in (2) comprises three terms representing amortized investment, maintenance, production, energy losses, and unserved energy costs. The first term corresponds to the present worth value of the expected investment cost under the assumption of a perpetual or infinite planning horizon [22]. The second term is the present value of the expected operating costs throughout the time span. Finally, the third term represents the present value of the expected operating costs incurred after the last time stage. As can be noted, this term relies on the operating costs at the last time stage and also assumes a perpetual planning horizon. The cost terms in (2) are formulated as follows:

$$\begin{aligned} c^I_t = &\sum_{l\in\{NRF,NAF\}} RR^l \sum_{k\in K^l}\sum_{(i,j)\in\Upsilon^l} C^{I,l}_k \ell_{ij} x^l_{ijkt} \\ &+ RR^{SS}\sum_{i\in\Psi^{SS}} C^{I,SS}_i x^{SS}_{it} \\ &+ RR^{NT}\sum_{k\in K^{NT}}\sum_{i\in\Psi^{SS}} C^{I,NT}_k x^{NT}_{ikt} \\ &+\sum_{p\in P} RR^p \sum_{k\in K^p}\sum_{i\in\Psi^p} C^{I,p}_k p f \bar{G}^p_k x^p_{ikt};\ \forall t\in T \end{aligned} \quad (3)$$

$$c_t^M = \sum_{l\in L}\sum_{k\in K^l}\sum_{(i,j)\in\Upsilon^l} C_k^{M,l}\left(y_{ijkt}^l + y_{jikt}^l\right) + \sum_{tr\in TR}\sum_{k\in K^{tr}}\sum_{i\in\Psi^{SS}} C_k^{M,tr} y_{ikt}^{tr} + \sum_{p\in P}\sum_{k\in K^p}\sum_{i\in\Psi^p} C_k^{M,p} y_{ikt}^p;\ \forall t\in T \quad (4)$$

$$c_t^E = \sum_{b\in B}\sum_{\omega=1}^{n_\Omega}\pi_b(\omega)\Delta_b pf\left(\sum_{tr\in TR}\sum_{k\in K^{tr}}\sum_{i\in\Psi^{SS}} C_b^{SS} g_{iktb}^{tr}(\omega) + \sum_{p\in P}\sum_{k\in K^p}\sum_{i\in\Psi^p} C_k^{E,p} g_{iktb}^p(\omega)\right);\ \forall t\in T \quad (5)$$

$$c_t^R = \sum_{b\in B}\sum_{\omega=1}^{n_\Omega}\pi_b(\omega)\Delta_b C_b^{SS} pf \left[\sum_{tr\in TR}\sum_{k\in K^{tr}}\sum_{i\in\Psi^{SS}} Z_k^{tr}\left(g_{iktb}^{tr}(\omega)\right)^2 + \sum_{l\in L}\sum_{k\in K^l}\sum_{(i,j)\in\Upsilon^l} Z_k^l \ell_{ij}\left(f_{ijktb}^l(\omega) + f_{jiktb}^l(\omega)\right)^2\right];\ \forall t\in T \quad (6)$$

$$c_t^U = \sum_{b\in B}\sum_{\omega=1}^{n_\Omega}\sum_{i\in\Psi_t^{LN}}\pi_b(\omega)\Delta_b C^U pf d_{itb}^U(\omega);\ \forall t\in T \quad (7)$$

where capital recovery rates are computed as $RR^l = (I(1+I)^{\eta^l})/((1+I)^{\eta^l}-1)$, $\forall l\in\{NRF, NAF\}$; $RR^{NT} = (I(1+I)^{\eta^{NT}})/((1+I)^{\eta^{NT}}-1)$; $RR^p = (I(1+I)^{\eta^p})/((1+I)^{\eta^p}-1)$, $\forall p\in P$; and $RR^{SS} = (I(1+I)^{\eta^{SS}})/((1+I)^{\eta^{SS}}-1)$.

It is worth emphasizing that, for each time stage, a single binary variable per conductor in the feeder connecting nodes i and j is used to model the associated investment decision, namely x_{ijkt}^l. In contrast, two binary variables, y_{ijkt}^l and y_{jikt}^l, as well as two continuous variables, $f_{ijktb}^l(\omega)$ and $f_{jiktb}^l(\omega)$, are associated with each feeder in order to model its utilization and current flow, respectively. Note that $f_{ijktb}^l(\omega)$ is greater than 0 and equal to the current flow through the feeder between nodes i and j measured at node i only when the current flows from i to j, being 0 otherwise.

In (3), the amortized investment cost at each stage is formulated as the sum of terms related to: (i) replacement and addition of feeders, (ii) reinforcement of existing substations and construction of new ones, (iii) installation of new transformers, and (iv) installation of generators. It should be emphasized that the investment cost for substations corresponds to the cost associated with the upgrading or construction of this infrastructure excluding the cost of transformers, which is explicitly considered in the third term of (3). Expressions (4) model the maintenance costs of feeders, transformers, and generators at each stage. The expected production costs associated with substations and generators are characterized in (5). Analogously, the expected costs of energy losses in feeders and transformers are modeled in (6). Similar to [16], [18], energy losses are formulated as quadratic terms. Such nonlinearities can be accurately approximated by a set of tangent lines, as explained in Section III-E. This approximation yields piecewise linear functions, which, for practical purposes, are indistinguishable from nonlinear models if enough segments are used. Finally, expressions (7) correspond to the penalty cost of the expected unserved energy.

B. Kirchhoff's Laws and Operational Limits

The constraints associated with the system operation are formulated as:

$$\underline{V} \le v_{itb}(\omega) \le \overline{V};\ \forall i\in\Psi^N,\ \forall t\in T,\ \forall b\in B,\ \forall\omega = 1\ldots n_\Omega \quad (8)$$

$$0 \le f_{ijktb}^l(\omega) \le y_{ijkt}^l \bar{F}_k^l;\ \forall l\in L,\ \forall i\in\Psi_j^l,\ \forall j\in\Psi^N,\ \forall k\in K^l,\ \forall t\in T,\ \forall b\in B,\ \forall\omega = 1\ldots n_\Omega \quad (9)$$

$$0 \le g_{iktb}^{tr}(\omega) \le y_{ikt}^{tr}\bar{G}_k^{tr};\ \forall tr\in TR,\ \forall i\in\Psi^{SS},\ \forall k\in K^{tr},\ \forall t\in T,\ \forall b\in B,\ \forall\omega = 1\ldots n_\Omega \quad (10)$$

$$0 \le d_{itb}^U(\omega) \le \mu_b^D(\omega) D_{it};\ \forall i\in\Psi_t^{LN},\ \forall t\in T,\ \forall b\in B,\ \forall\omega = 1\ldots n_\Omega \quad (11)$$

$$0 \le g_{iktb}^C(\omega) \le y_{ikt}^C \bar{G}_k^C;\ \forall i\in\Psi^C,\ \forall k\in K^C,\ \forall t\in T,\ \forall b\in B,\ \forall\omega = 1\ldots n_\Omega \quad (12)$$

$$0 \le g_{iktb}^p(\omega) \le y_{ikt}^p \hat{G}_{ikb}^p(\omega);\ \forall p\in\{W,\Theta\},\ \forall i\in\Psi^p,\ \forall k\in K^p,\ \forall t\in T,\ \forall b\in B,\ \forall\omega = 1\ldots n_\Omega \quad (13)$$

$$\sum_{p\in P}\sum_{k\in K^p}\sum_{i\in\Psi^p} g_{iktb}^p(\omega) \le \xi\sum_{i\in\Psi_t^{LN}}\mu_b^D(\omega) D_{it};\ \forall t\in T,\ \forall b\in B,\ \forall\omega = 1\ldots n_\Omega \quad (14)$$

$$\sum_{l\in L}\sum_{k\in K^l}\sum_{j\in\Psi_i^l}\left[f_{ijktb}^l(\omega) - f_{jiktb}^l(\omega)\right] = \sum_{tr\in TR}\sum_{k\in K^{tr}} g_{iktb}^{tr}(\omega) + \sum_{p\in P}\sum_{k\in K^p} g_{iktb}^p(\omega) - \mu_b^D(\omega) D_{it} + d_{itb}^U(\omega);\ \forall i\in\Psi^N,\ \forall t\in T,\ \forall b\in B,\ \forall\omega = 1\ldots n_\Omega \quad (15)$$

$$y_{ijkt}^l\left[Z_k^l \ell_{ij} f_{ijktb}^l(\omega) - (v_{itb}(\omega) - v_{jtb}(\omega))\right] = 0;\ \forall l\in L,\ \forall i\in\Psi_j^l,\ \forall j\in\Psi^N,\ \forall k\in K^l,\ \forall t\in T,\ \forall b\in B,\ \forall\omega = 1\ldots n_\Omega. \quad (16)$$

Constraints (8) set the bounds on the magnitudes of nodal voltages. Similarly, upper and lower limits on network- and generation-related variables are modeled in (9)–(13). DG penetration is limited in (14) as a ξ fraction of the demand. Finally, the effect of the distribution network is characterized in (15), (16) by a linearized network model that was first proposed by Haffner *et al.* [23] and successfully applied in [16], [18], [24]. Note that constraints (16) include nonlinearities involving the products of binary variables y_{ijkt}^l and continuous variables $f_{ijktb}^l(\omega)$ and $v_{itb}(\omega)$, for which a linear equivalent is provided in Section III-E.

C. Investment and Utilization Constraints

Investment and utilization decisions are constrained according to the following expressions:

$$x_{ijkt}^l \in\{0,1\};\ \forall l\in\{NRF, NAF\},\ \forall(i,j)\in\Upsilon^l,\ \forall k\in K^l,\ \forall t\in T \quad (17)$$

$$x_{it}^{SS} \in\{0,1\};\ \forall i\in\Psi^{SS},\ \forall t\in T \quad (18)$$

$$x_{ikt}^{NT} \in \{0,1\};\ \forall i \in \Psi^{SS},\ \forall k \in K^{NT},\ \forall t \in T \quad (19)$$

$$x_{ikt}^{p} \in \{0,1\};\ \forall p \in P,\ \forall i \in \Psi^{p},\ \forall k \in K^{p},\ \forall t \in T \quad (20)$$

$$y_{ijkt}^{l} \in \{0,1\};\ \forall l \in L,\ \forall i \in \Psi_j^{l},\ \forall j \in \Psi^{N},\ \forall k \in K^{l},\ \forall t \in T \quad (21)$$

$$y_{ikt}^{tr} \in \{0,1\};\ \forall tr \in TR,\ \forall i \in \Psi^{SS},\ \forall k \in K^{tr},\ \forall t \in T \quad (22)$$

$$y_{ikt}^{p} \in \{0,1\};\ \forall p \in P,\ \forall i \in \Psi^{p},\ \forall k \in K^{p},\ \forall t \in T \quad (23)$$

$$\sum_{t\in T}\sum_{k\in K^{l}} x_{ijkt}^{l} \le 1;\ \forall l \in \{NRF, NAF\},\ \forall (i,j) \in \Upsilon^{l} \quad (24)$$

$$\sum_{t\in T} x_{it}^{SS} \le 1;\ \forall i \in \Psi^{SS} \quad (25)$$

$$\sum_{t\in T}\sum_{k\in K^{NT}} x_{ikt}^{NT} \le 1;\ \forall i \in \Psi^{SS} \quad (26)$$

$$\sum_{t\in T}\sum_{k\in K^{p}} x_{ikt}^{p} \le 1;\ \forall p \in P,\ \forall i \in \Psi^{p} \quad (27)$$

$$x_{ikt}^{NT} \le \sum_{\tau=1}^{t} x_{i\tau}^{SS};\ \forall i \in \Psi^{SS},\ \forall k \in K^{NT},\ \forall t \in T \quad (28)$$

$$y_{ijkt}^{EFF} + y_{jikt}^{EFF} \le 1;\ \forall (i,j) \in \Upsilon^{SW,EFF},\ \forall k \in K^{EFF},\ \forall t \in T \quad (29)$$

$$y_{ijkt}^{l} + y_{jikt}^{l} \le \sum_{\tau=1}^{t} x_{ijk\tau}^{l};\ \forall l \in \{NRF, NAF\},\ \forall (i,j) \in \Upsilon^{SW,l},\ \forall k \in K^{l},\ \forall t \in T \quad (30)$$

$$y_{ijkt}^{ERF} + y_{jikt}^{ERF} \le 1 - \sum_{\tau=1}^{t}\sum_{\kappa\in K^{NRF}} x_{ij\kappa\tau}^{NRF};\ \forall (i,j) \in \Upsilon^{SW,ERF},\ \forall k \in K^{ERF},\ \forall t \in T \quad (31)$$

$$y_{ijkt}^{EFF} + y_{jikt}^{EFF} = 1;\ \forall (i,j) \in (\Upsilon^{EFF} \setminus \Upsilon^{SW,EFF}),\ \forall k \in K^{EFF},\ \forall t \in T \quad (32)$$

$$y_{ijkt}^{l} + y_{jikt}^{l} = \sum_{\tau=1}^{t} x_{ijk\tau}^{l};\ \forall l \in \{NRF, NAF\},\ \forall (i,j) \in (\Upsilon^{l} \setminus \Upsilon^{SW,l}),\ \forall k \in K^{l},\ \forall t \in T \quad (33)$$

$$y_{ijkt}^{ERF} + y_{jikt}^{ERF} = 1 - \sum_{\tau=1}^{t}\sum_{\kappa\in K^{NRF}} x_{ij\kappa\tau}^{NRF};\ \forall (i,j) \in (\Upsilon^{ERF} \setminus \Upsilon^{SW,ERF}),\ \forall k \in K^{ERF},\ \forall t \in T \quad (34)$$

$$y_{ikt}^{NT} \le \sum_{\tau=1}^{t} x_{ik\tau}^{NT};\ \forall i \in \Psi^{SS},\ \forall k \in K^{NT},\ \forall t \in T \quad (35)$$

$$y_{ikt}^{p} \le \sum_{\tau=1}^{t} x_{ik\tau}^{p};\ \forall p \in P, \forall i \in \Psi^{p}, \forall k \in K^{p}, \forall t \in T \quad (36)$$

$$\sum_{l\in\{NRF,NAF\}}\sum_{k\in K^{l}}\sum_{(i,j)\in\Upsilon^{l}} C_k^{I,l}\ell_{ij}x_{ijkt}^{l} + \sum_{i\in\Psi^{SS}} C_i^{I,SS}x_{it}^{SS} + \sum_{k\in K^{NT}}\sum_{i\in\Psi^{SS}} C_k^{I,NT}x_{ikt}^{NT} + \sum_{p\in P}\sum_{k\in K^{p}}\sum_{i\in\Psi^{p}} C_k^{I,p}pf\bar{G}_k^{p}x_{ikt}^{p} \le IB_t;\ \forall t \in T. \quad (37)$$

The binary nature of investment and utilization variables is imposed in (17)–(23). As per (24)–(27), a maximum of one reinforcement, replacement or addition is allowed for each system component and location along the planning horizon. Constraints (28) guarantee that new transformers can only be added in substations that have been previously expanded or built. Network reconfiguration constraints (29)–(31) model the utilization of feeders while explicitly characterizing the direction of current flows. Constraints (32)–(34) are analogous to (29)–(31) for the feeders that are not reconfigurable under normal operation. The utilization of new transformers is formulated in (35) whereas the utilization of newly installed generators is modeled in (36). Finally, constraints (37) impose a budgetary limit for investments at each stage.

D. Radiality Constraints

Radial operation is modeled by the following constraints:

$$\sum_{l\in L}\sum_{i\in\Psi_j^{l}}\sum_{k\in K^{l}} y_{ijkt}^{l} = 1;\ \forall j \in \Psi_t^{LN},\ \forall t \in T \quad (38)$$

$$\sum_{l\in L}\sum_{i\in\Psi_j^{l}}\sum_{k\in K^{l}} y_{ijkt}^{l} \le 1;\ \forall j \notin \Psi_t^{LN},\ \forall t \in T \quad (39)$$

$$\sum_{l\in L}\sum_{k\in K^{l}}\sum_{j\in\Psi_i^{l}} \left(\tilde{f}_{ijkt}^{l} - \tilde{f}_{jikt}^{l}\right) = \tilde{g}_{it}^{SS} - \tilde{D}_{it};\ \forall i \in \Psi^{N},\ \forall t \in T \quad (40)$$

$$0 \le \tilde{f}_{ijkt}^{EFF} \le n_{DG};\ \forall i \in \Psi_j^{EFF},\ \forall j \in \Psi^{N},\ \forall k \in K^{EFF},\ \forall t \in T \quad (41)$$

$$0 \le \tilde{f}_{ijkt}^{ERF} \le n_{DG}\left(1 - \sum_{\tau=1}^{t}\sum_{\kappa\in K^{NRF}} x_{ij\kappa\tau}^{NRF}\right);\ \forall (i,j) \in \Upsilon^{ERF},\ \forall k \in K^{ERF},\ \forall t \in T \quad (42)$$

$$0 \le \tilde{f}_{jikt}^{ERF} \le n_{DG}\left(1 - \sum_{\tau=1}^{t}\sum_{\kappa\in K^{NRF}} x_{ij\kappa\tau}^{NRF}\right);\ \forall (i,j) \in \Upsilon^{ERF},\ \forall k \in K^{ERF},\ \forall t \in T \quad (43)$$

$$0 \le \tilde{f}_{ijkt}^{l} \le n_{DG}\sum_{\tau=1}^{t} x_{ijk\tau}^{l};\ \forall l \in \{NRF, NAF\},\ \forall (i,j) \in \Upsilon^{l},\ \forall k \in K^{l},\ \forall t \in T \quad (44)$$

$$0 \le \tilde{f}_{jikt}^{l} \le n_{DG}\sum_{\tau=1}^{t} x_{ijk\tau}^{l};\ \forall l \in \{NRF, NAF\},\ \forall (i,j) \in \Upsilon^{l},\ \forall k \in K^{l},\ \forall t \in T \quad (45)$$

$$0 \le \tilde{g}_{it}^{SS} \le n_{DG};\ \forall i \in \Psi^{SS},\ \forall t \in T. \quad (46)$$

As done in [16], [18], constraints (38) impose load nodes to have a single input flow while expressions (39) set a maximum of one input flow for the remaining nodes. Based on the findings of [25], constraints (40)–(46), which model a fictitious system with fictitious demands, prevent DG islanding under normal operation while keeping radiality. Constraints (40) represent the nodal fictitious current balance equations where fictitious demands $\tilde{D}_{it}$ are defined as follows:

$$\tilde{D}_{it} = \begin{cases} 1; & \forall i \in \left((\Psi^{C} \cup \Psi^{W} \cup \Psi^{\Theta}) \cap \Psi_t^{LN}\right),\ \forall t \in T \\ 0; & \forall i \notin \left((\Psi^{C} \cup \Psi^{W} \cup \Psi^{\Theta}) \cap \Psi_t^{LN}\right),\ \forall t \in T. \end{cases} \quad (47)$$

Constraints (41)–(45) bound the fictitious flows through feeders. Finally, constraints (46) set the limits for the fictitious currents injected by the fictitious substations.

E. Mixed-Integer Linear Formulation

The proposed stochastic model is a mixed-integer nonlinear program that can be recast as an instance of mixed-integer linear programming by replacing nonlinear expressions (6) and (16) with linear terms.

Based on [26], a piecewise linear approximation is used for the quadratic terms in (6). Thus, expressions (6) are replaced with:

$$c_t^R = \sum_{b\in B}\sum_{\omega=1}^{n_\Omega}\pi_b(\omega)\Delta_b C_b^{SS} pf \left[\sum_{tr\in TR}\sum_{k\in K^{tr}}\sum_{i\in\Psi^{SS}}\sum_{h=1}^{n_H} M_{kh}^{tr}\delta_{iktbh}^{tr}(\omega) + \sum_{l\in L}\sum_{k\in K^l}\sum_{(i,j)\in\Upsilon^l}\sum_{h=1}^{n_H} M_{kh}^{l}\ell_{ij}\left(\delta_{ijktbh}^{l}(\omega)+\delta_{jiktbh}^{l}(\omega)\right)\right]; \quad \forall t\in T \tag{48}$$

$$g_{iktb}^{tr}(\omega) = \sum_{h=1}^{n_H}\delta_{iktbh}^{tr}(\omega);\ \forall tr\in TR,\ \forall i\in\Psi^{SS},\ \forall k\in K^{tr}, \quad \forall t\in T,\ \forall b\in B,\ \forall\omega=1\dots n_\Omega \tag{49}$$

$$0\le\delta_{iktbh}^{tr}(\omega)\le A_{kh}^{tr};\ \forall h=1\dots n_H,\ \forall tr\in TR, \quad \forall i\in\Psi^{SS},\ \forall k\in K^{tr},\ \forall t\in T,\ \forall b\in B,\ \forall\omega=1\dots n_\Omega \tag{50}$$

$$f_{ijktb}^{l}(\omega) = \sum_{h=1}^{n_H}\delta_{ijktbh}^{l}(\omega);\ \forall l\in L,\ \forall i\in\Psi_j^l, \quad \forall j\in\Psi^N,\ \forall k\in K^l,\ \forall t\in T,\ \forall b\in B,\ \forall\omega=1\dots n_\Omega \tag{51}$$

$$0\le\delta_{ijktbh}^{l}(\omega)\le A_{kh}^{l};\ \forall h=1\dots n_H,\ \forall l\in L,\ \forall i\in\Psi_j^l, \quad \forall j\in\Psi^N,\ \forall k\in K^l,\ \forall t\in T,\ \forall b\in B,\ \forall\omega=1\dots n_\Omega \tag{52}$$

where (48) are the linearized expected costs of energy losses, while (49), (50) and (51), (52) are related to the linearization of energy losses in transformers and feeders, respectively.

In addition, using the disjunctive-constraint-based transformation described in [27], nonlinear expressions (16) have the following linear equivalents:

$$\begin{aligned}&-J\left(1-y_{ijkt}^{l}\right)\\ &\le Z_k^l\ell_{ij}f_{ijktb}^{l}(\omega)-[v_{itb}(\omega)-v_{jtb}(\omega)]\\ &\le J\left(1-y_{ijkt}^{l}\right);\ \forall l\in L,\ \forall i\in\Psi_j^l,\ \forall j\in\Psi^N,\ \forall k\in K^l,\\ &\quad\forall t\in T,\ \forall b\in B,\ \forall\omega=1\dots n_\Omega.\end{aligned} \tag{53}$$

Thus, the resulting mixed-integer linear program is formulated as:

$$\underset{\substack{c_t^E,c_t^I,c_t^M,c_t^R,c^{TPV},c_t^U,d_{itb}^U(\omega),f_{ijktb}^l(\omega),\\ f_{ijkt}^l,g_{iktb}^p(\omega),g_{iktb}^{tr}(\omega),\tilde{g}_{it}^{SS},v_{itb}(\omega),\\ x_{ijkt}^l,x_{ikt}^{NT},x_{ikt}^p,x_{it}^{SS},y_{ijkt}^l,y_{ikt}^p,y_{ikt}^{tr},\\ \delta_{ijktbh}^l(\omega),\delta_{iktbh}^{tr}(\omega)}}{\text{Minimize}} \quad c^{TPV} \tag{54}$$

$$\begin{aligned}&\text{subject to:}\\ &\text{Constraints } (2)-(5),\ (7)-(15),\ (17)-(46),\\ &\quad\text{and } (48)-(53).\end{aligned} \tag{55}$$

IV. Reliability Calculation

Based on [13]–[16], [28], several reliability indices and their corresponding costs are calculated in order to quantitatively measure system reliability and its economic impact. This reliability assessment is based on an analytical contingency enumeration method [21] that considers continuity only and, hence, neglects power flows.

As done in [16], only sustained interruptions due to single outages are considered in the definition of the reliability indices. Such outages may be due to a fault in a feeder or to a contingency in the load node downstream. In addition, based on [8], reliability indices and their associated costs are computed for a particular loading condition and a given radially-operated network topology considering (i) failure rates of feeders and (ii) interruption durations, which depend on the repair and switching times.

According to [16], [29], [30], reliability indices are calculated on the basis of two assumptions, namely (i) each feeder connected to a substation has a circuit breaker without a recloser at the output of the substation, and (ii) each feeder has a switch that enables the reconfiguration of the system after a fault in order to meet the demand in the most efficient way. Thus, once a sustained fault has occurred, the first circuit breaker upstream the fault trips, thereby curtailing all load demands downstream. Subsequently, the system topology is reconfigured by operating switches and circuit breakers to reduce the non-supplied energy. To that end, the first switch upstream the fault is opened in order to isolate the fault. Then the circuit breaker is closed so that the supply to all load demands between the circuit breaker and the switch is restored. Finally, once the isolated fault is cleared, the corresponding switch is closed and complete service is reestablished.

Within this framework and according to the IEEE standards and application guides [31]–[33], intentional islanding of DG units under contingency is addressed. To that end, DG units are considered as negative loads that can be run under contingency, thereby improving system reliability due to the partial supply of the loads downstream the contingency, which would be otherwise completely curtailed. It should be noted that such operation of DG under contingency will play a key role in the future smart distribution grids. Thus, for the purposes of reliability calculation, the effect of uncertain load and DG is modeled as:

$$D_{itb}^{net}(\omega) = \max\left\{0, \mu_b^D(\omega)D_{it} - \sum_{k\in K^C}\bar{G}_k^C\sum_{\tau=1}^{t}\hat{x}_{ik\tau}^C - \sum_{p\in\{W,\Theta\}}\sum_{k\in K^p}\hat{G}_{ikb}^p(\omega)\sum_{\tau=1}^{t}\hat{x}_{ik\tau}^p\right\}; \quad \forall i\in\Psi_t^{LN},\ \forall t\in T,\ \forall b\in B,\ \forall\omega=1\dots n_\Omega. \tag{56}$$

This model explicitly considers investment decisions in DG. Moreover, for renewable-based DG, the model captures the effect of the intermittent energy sources on the availability of power generation. The benefit of further energy replacement by DG with energy capability exceeding the expected load demand of the node where it is connected would require the incorporation of a load flow model in the analytical method at the expense

of an increased computational effort. Notwithstanding, the proposed model provides a reasonable tradeoff between accuracy and computational burden for the purposes of multistage distribution system planning.

A. Reliability Indices

The following indices are the most commonly used metrics for distribution system reliability [2], [13]–[16]:

- Customer interruption frequency (CIF) at load node r and stage t:

$$CIF_{rt} = \sum_{\gamma\in\Gamma} \sum_{(i,j)\in\Upsilon_t | r\in\Psi^{\gamma}_{ijt}} \lambda_{ij}. \tag{57}$$

- Customer interruption duration (CID) at load node r and stage t:

$$CID_{rt} = \sum_{\gamma\in\Gamma} DI^{\gamma} \sum_{(i,j)\in\Upsilon_t | r\in\Psi^{\gamma}_{ijt}} \lambda_{ij}. \tag{58}$$

- System average interruption frequency index (SAIFI) for stage t:

$$SAIFI_t = \frac{\sum\limits_{(i,j)\in\Upsilon_t} \lambda_{ij} \sum\limits_{\gamma\in\Gamma} \sum\limits_{r\in\Psi^{\gamma}_{ijt}} NC_{rt}}{\sum\limits_{r\in\Psi^{N}} NC_{rt}}. \tag{59}$$

- System average interruption duration index (SAIDI) for stage t:

$$SAIDI_t = \frac{\sum\limits_{(i,j)\in\Upsilon_t} \lambda_{ij} \sum\limits_{\gamma\in\Gamma} DI^{\gamma} \sum\limits_{r\in\Psi^{\gamma}_{ijt}} NC_{rt}}{\sum\limits_{r\in\Psi^{N}} NC_{rt}}. \tag{60}$$

- Average system availability index (ASAI) for stage t:

$$ASAI_t = 1 - \frac{SAIDI_t}{8760}. \tag{61}$$

- Expected energy not supplied (EENS) for stage t:

$$EENS_t = \sum_{b\in B} \frac{\Delta_b}{8760} \sum_{i\in\Psi^{LN}_t} CID_{it} \sum_{\omega=1}^{n_\Omega} \pi_b(\omega) pfD^{net}_{itb}(\omega). \tag{62}$$

B. Reliability Costs

According to the aforementioned indices, several regulation-dependent costs of reliability can be defined [16] such as the cost of customer interruption (CIC), which accounts for both CIF and CID; the cost of system average interruption (SAIC); and the cost of expected energy not supplied (EENSC). As done in [16], here we assume that distribution companies compensate customers for the violation of reliability indices. This compensation is proportional to the violation level according to the cost of energy supplied by substations, C^{SS}_b, and to a penalty factor, χ, set by the regulator.

The customer interruption cost at stage t is:

$$CIC_t = \max\{CIFC_t, CIDC_t\} \tag{63}$$

where the costs related to CIF and CID are:

$$CIFC_t = \chi \left[\sum_{i\in\Psi^{LN}_t} \max\left\{0, (CIF_{it} - \overline{CIF}) \sum_{b\in B} \sum_{\omega=1}^{n_\Omega} \pi_b(\omega) \frac{\Delta_b}{8760} C^{SS}_b D^{net}_{itb}(\omega)\right\}\right] \tag{64}$$

$$CIDC_t = \chi \left[\sum_{i\in\Psi^{LN}_t} \max\left\{0, (CID_{it} - \overline{CID}) \sum_{b\in B} \sum_{\omega=1}^{n_\Omega} \pi_b(\omega) \frac{\Delta_b}{8760} C^{SS}_b D^{net}_{itb}(\omega)\right\}\right]. \tag{65}$$

The economic valuation of not complying with SAIFI or SAIDI at a specific stage is also regulation dependent. According to [16], we consider the penalty applied by the regulator as a percentage ς of the cost of the energy supplied by substations, C^{SS}_b. Thus, the cost of system average interruption at stage t is:

$$SAIC_t = \begin{cases} \varsigma \sum_{b\in B} \sum_{\omega=1}^{n_\Omega} \sum_{i\in\Psi^{LN}_t} \pi_b(\omega) \Delta_b C^{SS}_b D^{net}_{itb}(\omega); \\ \quad \text{if } SAIFI_t > \overline{SAIFI} \\ \quad \text{or } SAIDI_t > \overline{SAIDI} \\ 0, \text{ otherwise.} \end{cases} \tag{66}$$

Furthermore, the cost of the expected energy not supplied for stage t is calculated as follows:

$$EENSC_t = \sum_{b\in B} \frac{\Delta_b}{8760} C^{SS}_b \sum_{i\in\Psi^{LN}_t} CID_{it} \sum_{\omega=1}^{n_\Omega} \pi_b(\omega) pfD^{net}_{itb}(\omega). \tag{67}$$

In order to properly consider the aforementioned cost terms in the framework of multistage expansion planning, their present values, denoted by CIC^{PV}, $EENSC^{PV}$, and $SAIC^{PV}$, are calculated under the same assumptions adopted for the operating cost terms in (2).

V. Proposed Algorithm

The proposed algorithm relies on the generation of a pool of cheap candidate expansion plans in terms of investment and operational costs. For each expansion plan, reliability indices and their associated costs are subsequently computed. The information on investment, operational, and reliability costs allows the distribution planner to make informed decisions on the most suitable expansion plan. The proposed planning algorithm consists of the following steps:

Step 1) Obtain a pool of solutions with different topologies by iteratively solving the expansion planning problem described in Section III. At each iteration m, a non-redundancy constraint [34] is added to the optimization problem as follows:

$$\sum_{(i,j)\in\Lambda^{1(\varrho)}} \left(1 - \sum_{k\in K^{NAF}} \sum_{t\in T} x^{NAF}_{ijkt}\right) + \sum_{(i,j)\in\Lambda^{0(\varrho)}} \left(\sum_{k\in K^{NAF}} \sum_{t\in T} x^{NAF}_{ijkt}\right) \geq n_d;\ \forall \varrho = 1 \ldots m-1 \tag{68}$$

where $\Lambda^{1(\varrho)} = \{(i,j) \in \Upsilon^{NAF} | (\sum_{k\in K^{NAF}} \sum_{t\in T} x_{ijkt}^{NAF(\varrho)} = 1)\}$ and $\Lambda^{0(\varrho)} = \{(i,j) \in \Upsilon^{NAF} | (\sum_{k\in K^{NAF}} \sum_{t\in T} x_{ijkt}^{NAF(\varrho)} = 0)\}$. Constraints (68) allow us to obtain a new expansion plan at each iteration that differs from the previous plans in the topology at the last stage. At each iteration ϱ, $\Lambda^{1(\varrho)}$ stores the branches with candidate feeders for addition where investments have been made. Analogously, $\Lambda^{0(\varrho)}$ includes the branches with candidate feeders for addition where no expansion has been planned. Moreover, n_d denotes the minimum number of investments in newly added feeders by which the new expansion plan at each iteration differs from previous solutions.

Step 2) According to Section IV-A, compute the reliability indices associated with each expansion plan resulting from step 1.

Step 3) According to Section IV-B, calculate the reliability costs associated with each expansion plan resulting from step 1.

Step 4) Select the investment plan on the basis of the comparison of the topologies of the different solutions of the pool and the consideration of the associated costs.

VI. Numerical Results

This section presents and discusses results from three different case studies over a ten-year planning horizon. The proposed algorithm has first been applied to an insular distribution system based on the 54-node benchmark presented in [35]. Subsequently, the scalability of the proposed approach is validated with two case studies comprising 86 and 138 nodes, which are modified versions of those described in [18] and [36], respectively. Based on extensive numerical testing, four time blocks are considered and the cumulative distribution functions for demand, wind speed, and solar irradiation factors are all divided into three equiprobable segments. Thus, according to the procedure described in Section II, 27 equiprobable scenarios are generated for each time block, thereby totaling 108 scenarios per stage. For reproducibility puposes, data for the three case studies can be donwloaded from [37], where the currency used is U.S. dollars, hereinafter denoted by $.

Simulations have been implemented on a Dell PowerEdge R920X64 with four Intel Xeon E7-4820 processors at 2.00 GHz and 768 GB of RAM using CPLEX 12.6 [20] and GAMS 24.2 [38]. For the three case studies, the algorithm has been run for six iterations with parameter n_d equal to 10 so that six sufficiently different solutions are obtained. For each iteration, the stopping criterion for the branch-and-cut algorithm of CPLEX is based on an optimality gap equal to 1%.

A. 54-Node Case Study

The system comprises 50 load nodes, 4 substation nodes, and 63 branches. Tables II and III provide cost information for the six solutions, which were attained in 8.7 h on average. Table II shows the present value of the expected investment, maintenance, production, losses, and unserved energy costs.

TABLE II
54-Node System—Present Value of Investment and Operational Costs With DG (10^6 $)

Costs	Solution					
	1	2	3	4	5	6
Investment	15.56	17.46	13.56	12.43	13.62	16.78
Maintenance	5.89	6.98	5.00	4.43	4.87	6.45
Production	276.38	272.70	279.07	280.93	279.42	274.59
Losses	8.90	8.99	8.92	9.59	9.09	9.67
Unserved energy	0.58	1.59	1.35	0.58	1.10	0.67
Total	307.31	307.72	307.90	307.96	308.10	308.16

TABLE III
54-Node System—Present Value of Reliability Costs With DG (10^6 $)

	Solution					
	1	2	3	4	5	6
CIC^{PV}	0.027	0.036	0.017	0.024	0.043	0.036
$SAIC^{PV}$	2.225	2.220	0.168	2.424	2.068	2.700
$EENSC^{PV}$	0.077	0.078	0.077	0.081	0.078	0.082

Note that the topological and investment differences among solutions yield slight variations under 0.28% in the present value of the total cost. Table III lists the present value of the reliability costs described in Section IV. For this particular case study, the most relevant cost is $SAIC^{PV}$ since it is two orders of magnitude larger than CIC^{PV} and $EENSC^{PV}$. Besides, no significant differences across solutions can be found for $EENSC^{PV}$.

The results presented in Tables II and III reveal that Solution 1 outperforms Solutions 2, 4, and 6 since, in general, lower total costs are incurred. Analogously, it can be seen that Solution 3 outperforms Solutions 4, 5, and 6 in terms of both investment and operational costs and reliability costs. Thus, Solutions 2, 4, 5, and 6 are discarded by the planner. For the remaining solutions, the results presented in Table II show that Solution 1 is cheaper than Solution 3 by $0.59 million when reliability is disregarded. From Table III it can be observed that $SAIC^{PV}$ for Solution 3 is $2.057 million lower than that for Solution 1. Hence, this reduction in $SAIC^{PV}$ outweighs the larger investment and operational costs associated with Solution 3, so that Solution 1 is also discarded by the planner. Therefore, for this case, despite not being the first solution identified by the iterative algorithm, Solution 3 is the most suitable expansion plan taking into account both economic and reliability aspects. It is worth mentioning that Solution 3 attains a significant 92.45% reduction in $SAIC^{PV}$ over Solution 1 while slightly increasing investment and operational costs by 0.19%.

In order to numerically substantiate the beneficial impact of DG on both investment and operational costs and reliability costs, we have solved the expansion planning problem disregarding DG for the radially-operated network topologies of Solutions 1–6. This simpler expansion planning problem is identical to that addressed in [16]. Tables IV and V summarize the economic results for all solutions. Table IV shows the present value of the expected investment, maintenance, production, losses, and unserved energy costs. As expected for each solution, lower investment and maintenance costs are incurred

TABLE IV
54-NODE SYSTEM—PRESENT VALUE OF INVESTMENT AND OPERATIONAL COSTS WITHOUT DG RESULTING FROM [16] (10^6 $)

Costs	Solution					
	1	2	3	4	5	6
Investment	3.30	2.84	3.39	3.02	2.79	2.97
Maintenance	0.28	0.26	0.29	0.28	0.27	0.28
Production	293.51	293.46	293.45	293.18	292.79	292.89
Losses	10.00	10.54	9.52	10.09	10.04	10.70
Unserved energy	1.64	2.01	2.03	3.23	4.95	4.39
Total	308.73	309.11	308.68	309.80	310.84	311.23

TABLE V
54-NODE SYSTEM—PRESENT VALUE OF RELIABILITY COSTS WITHOUT DG RESULTING FROM [16] (10^6 $)

	Solution					
	1	2	3	4	5	6
CIC^{PV}	0.027	0.036	0.017	0.024	0.052	0.036
$SAIC^{PV}$	2.332	2.332	0.172	2.506	2.157	2.824
$EENSC^{PV}$	0.079	0.082	0.078	0.083	0.081	0.085

as compared to the case with DG. However, the increase in production, energy losses, and unserved energy costs is greater than this reduction, thereby resulting in moderately higher total costs with increase factors ranging between 0.25% for Solution 3 and 1.00% for Solution 6. This moderate cost increase is a consequence of the unmodified topology with respect to that identified by the expansion planning with DG. However, such seemingly minor impact in terms of investment and operational costs has a substantial effect on reliability. Table V lists the present value of the costs associated with reliability. As can be seen, reliability costs for all solutions are greater than or equal to those considering DG (Table III). In particular, $SAIC^{PV}$, which is the most relevant cost, is increased by factors ranging between 2.38% for Solution 3 and 5.05% for Solution 2. Thus, these results show that the incorporation of DG in distribution system planning yields better solutions in terms of both investment and operational costs and reliability costs.

For comparison purposes, we have also applied the methodology presented in [8], where scenarios were solved separately. The best solution provided by this approach is characterized by a present value of the total investment and operational cost equal to \$352.52 million and a null $SAIC^{PV}$, which is the most representative cost of reliability. This result corroborates the superiority of our proposed approach based on the simultaneous consideration of all scenarios according to standard stochastic programming [12]. Note that the best solution identified by our two-step algorithm (Solution 3 of Tables II and III) yields a significant reduction in investment and operational cost of \$44.62 million while the reliability cost experiences a slight increase of \$0.168 million.

B. 86-Node Case Study

The system comprises 83 load nodes, 3 substation nodes, and 94 branches. Tables VI and VII present the results associated with each candidate solution, which required 12.5 h on average. As can be seen, despite not being the best candidate solution found by the iterative algorithm disregarding reliability costs, Solution 3 is the best expansion plan in terms of both investment and operational costs and reliability costs. This fact shows the significant impact that reliability has on distribution system planning.

TABLE VI
86-NODE SYSTEM—PRESENT VALUE OF INVESTMENT AND OPERATIONAL COSTS (10^6 $)

Costs	Solution					
	1	2	3	4	5	6
Investment	10.30	11.93	12.58	11.45	14.01	12.58
Maintenance	4.44	5.02	5.40	4.94	6.20	5.30
Production	215.66	213.81	212.67	213.83	211.20	213.64
Losses	5.29	5.13	4.98	4.96	5.06	5.43
Unserved energy	0.26	0.32	0.58	1.04	0.33	0.15
Total	235.95	236.21	236.21	236.22	236.80	237.10

TABLE VII
86-NODE SYSTEM—PRESENT VALUE OF RELIABILITY COSTS (10^6 $)

	Solution					
	1	2	3	4	5	6
CIC^{PV}	0.072	0.068	0.060	0.060	0.073	0.092
$SAIC^{PV}$	1.744	1.623	0.000	0.000	1.869	1.890
$EENSC^{PV}$	0.067	0.065	0.060	0.060	0.066	0.067

TABLE VIII
138-NODE SYSTEM—PRESENT VALUE OF INVESTMENT AND OPERATIONAL COSTS (10^6 $)

Costs	Solution					
	1	2	3	4	5	6
Investment	3.53	10.16	8.07	9.53	7.75	13.23
Maintenance	0.67	4.12	3.07	3.90	2.96	5.26
Production	256.72	245.65	248.96	246.22	249.25	242.24
Losses	5.31	5.31	5.37	5.40	5.41	5.10
Unserved energy	0.04	1.29	1.25	1.84	1.59	1.15
Total	266.27	266.53	266.72	266.89	266.96	266.98

TABLE IX
138-NODE SYSTEM—PRESENT VALUE OF RELIABILITY COSTS (10^6 $)

	Solution					
	1	2	3	4	5	6
CIC^{PV}	0.041	0.035	0.042	0.035	0.049	0.044
$SAIC^{PV}$	2.213	0.000	1.852	0.000	2.167	2.152
$EENSC^{PV}$	0.072	0.070	0.072	0.070	0.072	0.072

C. 138-Node Case Study

The system comprises 135 load nodes, 3 substation nodes, and 151 branches. Tables VIII and IX summarize the results associated with each candidate solution, which required 16 h on average. Bearing in mind that computational issues are not a primary concern in this kind of planning problem, the attainment of high-quality near-optimal solutions with moderate computational effort reveals the effectiveness of the proposed approach. Following the above decision-making process, Solution 2 is selected as the most suitable expansion plan. It is worth mentioning that Solution 2 is not the first solution identified by the iterative algorithm, thereby evidencing the need for accounting for reliability.

VII. Conclusions

In this paper, we have addressed the incorporation of uncertainty and reliability in the joint expansion planning of distribution network assets and DG. In the absence of mathematical-programming-based approaches considering both economic and reliability aspects in co-optimized distribution system planning under uncertainty, this paper presents a novel approach combining stochastic programming, mixed-integer linear programming, and predictive reliability assessment. The proposed methodology provides the distribution planner with a pool of cost-effective candidate expansion plans characterized by their corresponding reliability indices and costs. Thus, investment and operational costs can be balanced versus reliability of supply.

Numerical results illustrate the need for quantifying the impact of reliability on the decision-making problem faced by the distribution planner. This impact may lead to selecting an expansion plan different from that with minimum investment and operational costs.

It should be noted that the proposed approach is readily applicable to incorporate other practical aspects for the expansion planning of smart distribution grids such as storage devices and demand response. Such extension would require additional investment-related and operational constraints as well as some extra notation to properly index variables and parameters. We recognize that the extended model needs further numerical studies.

Ongoing research is devoted to explicitly modeling reliability as part of the formulation of the optimization problem, thereby avoiding the need for *ex-post* calculation based on contingency enumeration. Further work will address the issues brought up by DG on the dynamic performance side. Research will also be conducted to incorporate the effect of generation outages, demand response, electric vehicles, and storage devices.

References

[1] H. L. Willis, *Power Distribution Planning Reference Book*, 2nd ed. New York, NY, USA: Marcel Dekker, 2004.

[2] A. A. Chowdhury and D. O. Koval, "Current practices and customer value-based distribution system reliability planning," *IEEE Trans. Ind. Appl.*, vol. 40, no. 5, pp. 1174–1182, Sep./Oct. 2004.

[3] P. S. Georgilakis and N. D. Hatziargyriou, "A review of power distribution planning in the modern power systems era: Models, methods and future research," *Electr. Power Syst. Res.*, vol. 121, pp. 89–100, Apr. 2015.

[4] N. Jenkins, R. Allan, P. Crossley, D. Kirschen, and G. Strbac, *Embedded Generation*. London, UK: The Institution of Engineering and Technology, 2000.

[5] A. Keane, L. F. Ochoa, C. L. T. Borges, G. W. Ault, A. D. Alarcon-Rodriguez, R. A. F. Currie, F. Pilo, C. Dent, and G. P. Harrison, "State-of-the-art techniques and challenges ahead for distributed generation planning and optimization," *IEEE Trans. Power Syst.*, vol. 28, no. 2, pp. 1493–1502, May 2013.

[6] D. Zhu, R. P. Broadwater, K.-S. Tam, R. Seguin, and H. Asgeirsson, "Impact of DG placement on reliability and efficiency with time-varying loads," *IEEE Trans. Power Syst.*, vol. 21, no. 1, pp. 419–427, Feb. 2006.

[7] G. Celli, E. Ghiani, S. Mocci, and F. Pilo, "A multiobjective evolutionary algorithm for the sizing and siting of distributed generation," *IEEE Trans. Power Syst.*, vol. 20, no. 2, pp. 750–757, May 2005.

[8] C. L. T. Borges and V. F. Martins, "Multistage expansion planning for active distribution networks under demand and distributed generation uncertainties," *Int. J. Electr. Power Energy Syst.*, vol. 36, no. 1, pp. 107–116, Mar. 2012.

[9] M. F. Shaaban, Y. M. Atwa, and E. F. El-Saadany, "DG allocation for benefit maximization in distribution networks," *IEEE Trans. Power Syst.*, vol. 28, no. 2, pp. 639–649, May 2013.

[10] M. E. Samper and A. Vargas, "Investment decisions in distribution networks under uncertainty with distributed generation—Part I: Model formulation," *IEEE Trans. Power Syst.*, vol. 28, no. 3, pp. 2331–2340, Aug. 2013.

[11] M. E. Samper and A. Vargas, "Investment decisions in distribution networks under uncertainty with distributed generation—Part II: Implementation and results," *IEEE Trans. Power Syst.*, vol. 28, no. 3, pp. 2341–2351, Aug. 2013.

[12] J. R. Birge and F. Louveaux, *Introduction to Stochastic Programming*, 2nd ed. New York, NY, USA: Springer, 2011.

[13] R. Billinton and J. E. Billinton, "Distribution system reliability indices," *IEEE Trans. Power Deliv.*, vol. 4, no. 1, pp. 561–568, Jan. 1989.

[14] *IEEE Guide for Electric Power Distribution Reliability Indices*, IEEE Standard 1366-2003, May 2004.

[15] R. E. Brown, *Electric Power Distribution Reliability*, 2nd ed. Boca Raton, FL, USA: CRC Press, 2008.

[16] R. C. Lotero and J. Contreras, "Distribution system planning with reliability," *IEEE Trans. Power Deliv.*, vol. 26, no. 4, pp. 2552–2562, Oct. 2011.

[17] L. Baringo and A. J. Conejo, "Wind power investment within a market environment," *Appl. Energy*, vol. 88, no. 9, pp. 3239–3247, Sep. 2011.

[18] G. Muñoz-Delgado, J. Contreras, and J. M. Arroyo, "Joint expansion planning of distributed generation and distribution networks," *IEEE Trans. Power Syst.*, vol. 30, no. 5, pp. 2579–2590, Sep. 2015.

[19] G. L. Nemhauser and L. A. Wolsey, *Integer and Combinatorial Optimization*. New York, NY, USA: Wiley-Interscience, 1999.

[20] IBM ILOG CPLEX, 2015 [Online]. Available: http://www-01.ibm.com/software/commerce/optimization/cplex-optimizer

[21] R. E. Brown and A. P. Hanson, "Impact of two-stage service restoration on distribution reliability," *IEEE Trans. Power Syst.*, vol. 16, no. 4, pp. 624–629, Nov. 2001.

[22] L. Blank and A. Tarquin, *Engineering Economy*, 7th ed. New York, NY, USA: McGraw-Hill, 2012.

[23] S. Haffner, L. F. A. Pereira, L. A. Pereira, and L. S. Barreto, "Multistage model for distribution expansion planning with distributed generation—Part I: Problem formulation," *IEEE Trans. Power Del.*, vol. 23, no. 2, pp. 915–923, Apr. 2008.

[24] S. Haffner, L. F. A. Pereira, L. A. Pereira, and L. S. Barreto, "Multistage model for distribution expansion planning with distributed generation—Part II: Numerical results," *IEEE Trans. Power Del.*, vol. 23, no. 2, pp. 924–929, Apr. 2008.

[25] M. Lavorato, J. F. Franco, M. J. Rider, and R. Romero, "Imposing radiality constraints in distribution system optimization problems," *IEEE Trans. Power Syst.*, vol. 27, no. 1, pp. 172–180, Feb. 2012.

[26] S. P. Bradley, A. C. Hax, and T. L. Magnanti, *Applied Mathematical Programming*. Reading, MA, USA: Addison-Wesley, 1977.

[27] S. Binato, M. V. F. Pereira, and S. Granville, "A new Benders decomposition approach to solve power transmission network design problems," *IEEE Trans. Power Syst.*, vol. 16, no. 2, pp. 235–240, May 2001.

[28] A. A. Chowdhury and D. O. Koval, *Power Distribution System Reliability. Practical Methods and Applications*. Hoboken, NJ, USA: John Wiley & Sons, Inc., 2009.

[29] Y. Tang, "Power distribution system planning with reliability modeling and optimization," *IEEE Trans. Power Syst.*, vol. 11, no. 1, pp. 181–189, Feb. 1996.

[30] J.-H. Teng, Y.-H. Liu, C.-Y. Chen, and C.-F. Chen, "Value-based distributed generator placements for service quality improvements," *Int. J. Electr. Power Energy Syst.*, vol. 29, no. 3, pp. 268–274, Mar. 2007.

[31] *IEEE Standard for Interconnecting Distributed Resources with Electric Power Systems*, IEEE Standard 1547-2003, Jul. 2003.

[32] *IEEE Application Guide for IEEE Std 1547, IEEE Standard for Interconnecting Distributed Resources with Electric Power Systems*, IEEE Standard 1547.2-2008, Apr. 2009.

[33] *IEEE Guide for Design, Operation, Integration of Distributed Resource Island Systems with Electric Power Systems*, IEEE Standard 1547.4-2011, Jul. 2011.

[34] E. Balas and R. Jeroslow, "Canonical cuts on the unit hypercube," *SIAM J. Appl. Math.*, vol. 23, no. 1, pp. 61–69, Jul. 1972.

[35] V. Miranda, J. V. Ranito, and L. M. Proença, "Genetic algorithms in optimal multistage distribution network planning," *IEEE Trans. Power Syst.*, vol. 9, no. 4, pp. 1927–1933, Nov. 1994.

[36] C.-T. Su and C.-S. Lee, "Network reconfiguration of distribution systems using improved mixed-integer hybrid differential evolution," *IEEE Trans. Power Deliv.*, vol. 18, no. 3, pp. 1022–1027, Jul. 2003.

[37] G. Muñoz-Delgado, J. Contreras, and J. M. Arroyo, "Multistage generation and network expansion planning in distribution systems considering uncertainty and reliability: Data for case studies," [Online]. Available: https://drive.google.com/file/d/0B5Wja2Owv_j4YUtEeXVLTlZJSVU/view?usp=sharing
[38] GAMS Development Corporation, 2015 [Online]. Available: http://www.gams.com

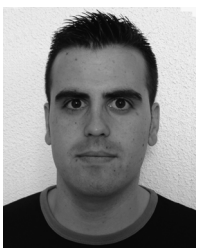

Gregorio Muñoz-Delgado (S'14) received the Ingeniero Industrial degree and the M.Sc. degree from the Universidad de Castilla-La Mancha, Ciudad Real, Spain, in 2012 and 2013, respectively. He is currently pursuing the Ph.D. degree at the Universidad de Castilla-La Mancha.

His research interests are in the fields of power systems planning, operations, and economics.

Javier Contreras (SM'05–F'15) received the B.S. degree in electrical engineering from the University of Zaragoza, Zaragoza, Spain, in 1989, the M.Sc. degree from the University of Southern California, Los Angeles, CA, USA, in 1992, and the Ph.D. degree from the University of California, Berkeley, CA, USA, in 1997.

He is a Professor at the Universidad de Castilla-La Mancha, Ciudad Real, Spain. His research interests include power systems planning, operations, and economics, as well as electricity markets.

José M. Arroyo (S'96–M'01–SM'06) received the Ingeniero Industrial degree from the Universidad de Málaga, Málaga, Spain, in 1995, and the Ph.D. degree in power systems operations planning from the Universidad de Castilla-La Mancha, Ciudad Real, Spain, in 2000.

From June 2003 through July 2004, he held a Richard H. Tomlinson Postdoctoral Fellowship at the Department of Electrical and Computer Engineering of McGill University, Montreal, QC, Canada. He is currently a Full Professor of electrical engineering at the Universidad de Castilla-La Mancha. His research interests include operations, planning, and economics of power systems, as well as optimization and parallel computation.